NASA TECHNICAL NOTE

NASA TN D-2595

NASA TN D-2595

EXPERIMENTAL LOCAL HEAT-TRANSFER DATA FOR PRECOOLED HYDROGEN AND HELIUM AT SURFACE TEMPERATURES UP TO 5300° R

by Maynard F. Taylor

Lewis Research Center

Cleveland, Ohio

NATIONAL AERONAUTICS AND SPACE ADMINISTRATION • WASHINGTON, D. C. • JANUARY 1965

EXPERIMENTAL LOCAL HEAT-TRANSFER DATA FOR PRECOOLED HYDROGEN AND HELIUM AT SURFACE TEMPERATURES UP TO 5300° R

By Maynard F. Taylor

Lewis Research Center
Cleveland, Ohio

NATIONAL AERONAUTICS AND SPACE ADMINISTRATION

For sale by the Office of Technical Services, Department of Commerce,
Washington, D.C. 20230 -- Price $1.00

EXPERIMENTAL LOCAL HEAT-TRANSFER DATA FOR

PRECOOLED HYDROGEN AND HELIUM AT

SURFACE TEMPERATURES UP TO 5300° R

by Maynard F. Taylor

Lewis Research Center

SUMMARY

14560

Local values of heat-transfer coefficients and average friction coefficients were measured experimentally for precooled hydrogen and helium gases flowing through an electrically heated tungsten tube with a length-diameter ratio of 77 for the following range of conditions: local surface temperatures up to 5300° R, inlet gas temperatures from 252° to 325° R, inlet pressures from 37 to 93 pounds per square inch absolute, local bulk Reynolds numbers from 5700 to 48,400, local ratios of surface to bulk gas temperature up to 8, and local heat fluxes up to 2,370,000 Btu per hour per square foot.

A comparison of several methods of correlating local heat-transfer coefficients was made for several types of wall temperature distributions, and one method was found to work exceedingly well in correlating hydrogen and helium data with surface to bulk gas temperature ratios up to 8.

Average friction coefficients for both helium and hydrogen are compared with the Kármán-Nikuradse relation.

Author

INTRODUCTION

One very interesting and important problem encountered in the proposed use of a nuclear reactor to heat hydrogen to propel a rocket is the effect of large property variations of the gas on its heat-transfer characteristics. The variations can be due to dissociation of the fluid or to large differences between surface and bulk gas temperatures or both. The ratio of surface to gas temperature can be as high as 25 at the inlet of a nuclear reactor if, for example, the surface temperature is 5000° R and the inlet gas temperature is 200° R. Some degree of dissociation will occur in the fluid adjacent to the fueled surface through most of the reactor and will occur in the bulk hydrogen at the reactor outlet. The effect of the large variations in the thermodynamic and transport properties on the heat-transfer characteristics of hydrogen is very important in the design considerations for nuclear-rocket-powered space vehicles.

TABLE I. - TEST CONDITIONS FROM VARIOUS SOURCES OF DATA

Source	Tube length-diameter ratio	Maximum surface to bulk temperature ratio	Maximum local surface temperature, °R	Maximum average surface temperature, °R	Inlet pressure, $\frac{lb}{sq\ in.}$ abs	Heat-transfer fluid	Types of heat-transfer coefficient measured
Ref. 1	30 to 120	3.5	----	3050	---	Air	Average
Ref. 2	20.9 to 42.6	11.09	----	2240	250	Helium and hydrogen	Local
Ref. 3	250	4.5	2300	----	250 to 1000	Helium and hydrogen	Local
Ref. 4	389	1.39	5040	3900	500 to 1500	Helium	Local and average
Ref. 5	60 and 92	3.9	5900	4533	40	Helium	Local and average
Ref. 6	77	5.6	5600	4749	40 to 100	Helium and hydrogen	Local
(a)	23.2	4.52	4600	----	110 to 850	Helium and hydrogen	Average
Present investigation	77	8.0	5300	4483	37 to 93	Helium and hydrogen	Local

[a]Unpublished data from Herbert J. Newman of Los Alamos Scientific Laboratory.

Reference 1 presents considerable data showing the effect of surface to fluid temperature ratio on the heat-transfer coefficient for air. Other investigations using helium and hydrogen and extending the range of surface to fluid temperature ratio (refs. 2 and 3) or the range of wall temperature (ref. 4) or both (refs. 5 and 6) have been presented. The conditions for which data were obtained in references 1 to 6 and in the present investigation are presented in table I. Reference 3 used an Inconel test section and lowered the inlet gas temperature with a liquid nitrogen bath. The melting point of Inconel limited the wall to fluid bulk temperature ratio to 4.5 in reference 3, while the room temperature inlet gas and the melting point of the tungsten test section limited the wall to bulk temperature ratio to 5.6 in reference 6. In the present investigation, a tungsten test section was used to obtain high wall temperatures, while the inlet gas temperature was lowered with liquid nitrogen to obtain surface to bulk fluid temperature ratios as high as 8. The experimental heat-transfer data from the present investigation are presented along with a recommended method for correlation.

EXPERIMENTAL APPARATUS

The test apparatus, test section, and instrumentation were the same as that described in reference 6 except that a liquid-nitrogen precooler was added to the inlet gas line as shown in figure 1. The precooler consisted of a 30-gallon stainless-steel tank in which a nine-turn coil of copper tubing was immersed in liquid nitrogen. The liquid level was held constant with a float switch. The tank was insulated with plastic foam.

The test section was fabricated and instrumented in the same manner as the one used in reference 6. The tungsten test section used in this experiment had

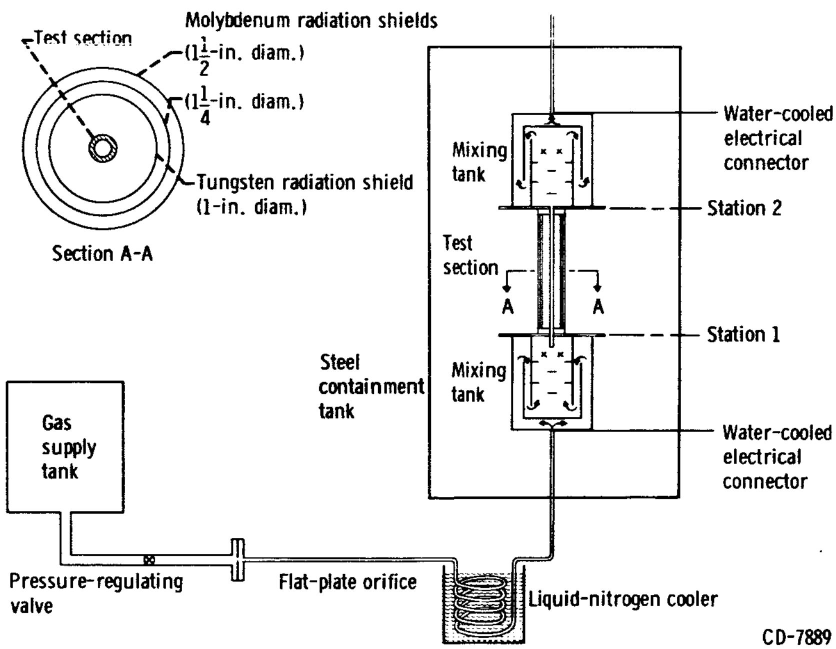

Figure 1. - Schematic diagram of arrangement of test apparatus.

an inside diameter of 0.115 inch, a heat-transfer length of 9 inches, and an entrance length of 14 diameters. The inlet gas temperature was measured with copper-constantan thermocouples with a liquid-nitrogen cold junction.

METHOD OF CALCULATION

The chemically frozen (chemical reaction term not included) transport and thermodynamic properties of hydrogen and helium used in the calculations of the heat-transfer and friction coefficients in this investigation were precisely the same as those used in reference 6, as were the physical properties of tungsten and molybdenum.

The average friction and local heat-transfer coefficients were calculated by the method used in reference 6. Local heat-transfer coefficients were approximated by dividing the test-section length into 10 equal increments and evaluating average coefficients for those small increments. Coefficients for the first and last increment were not used because of the large end losses.

RESULTS AND DISCUSSION

Axial Wall Temperature Distributions

Four axial outside wall temperature distributions, two for uncooled inlet gas and two for precooled inlet gas, are shown in figure 2 as a function of distance from the test-section entrance. Temperature measurements, including thermocouple and optical pyrometer readings for each run, are also shown. Experimental data including local h, T_b, and T_W for runs 1 to 23 (uncooled runs) are listed in table II of reference 6, while runs 32 to 52 (precooled runs) are summarized in table II of this report. (All symbols are defined in the appendix.) Figure 2 contains a comparison of run 17 with run 51 and run 18 with run 52. The runs compared have the same flow rate and maximum wall temperature. It can be seen from figure 2 that there is an increase in the surface temperature near the entrance of the tube for the runs with cooled inlet gas over that of the runs where the inlet gas is not cooled. The increase is a result of two factors. First, the ratio of surface to bulk fluid temperature is increased by lowering the fluid temperature. This is accompanied by a decrease in the heat-transfer coefficient, which tends to increase the surface temperature further. Second, the effect of increasing the ratio of surface to bulk fluid temperature is magnified by the increased electrical resistivity of tungsten at higher temperatures. The large axial temperature

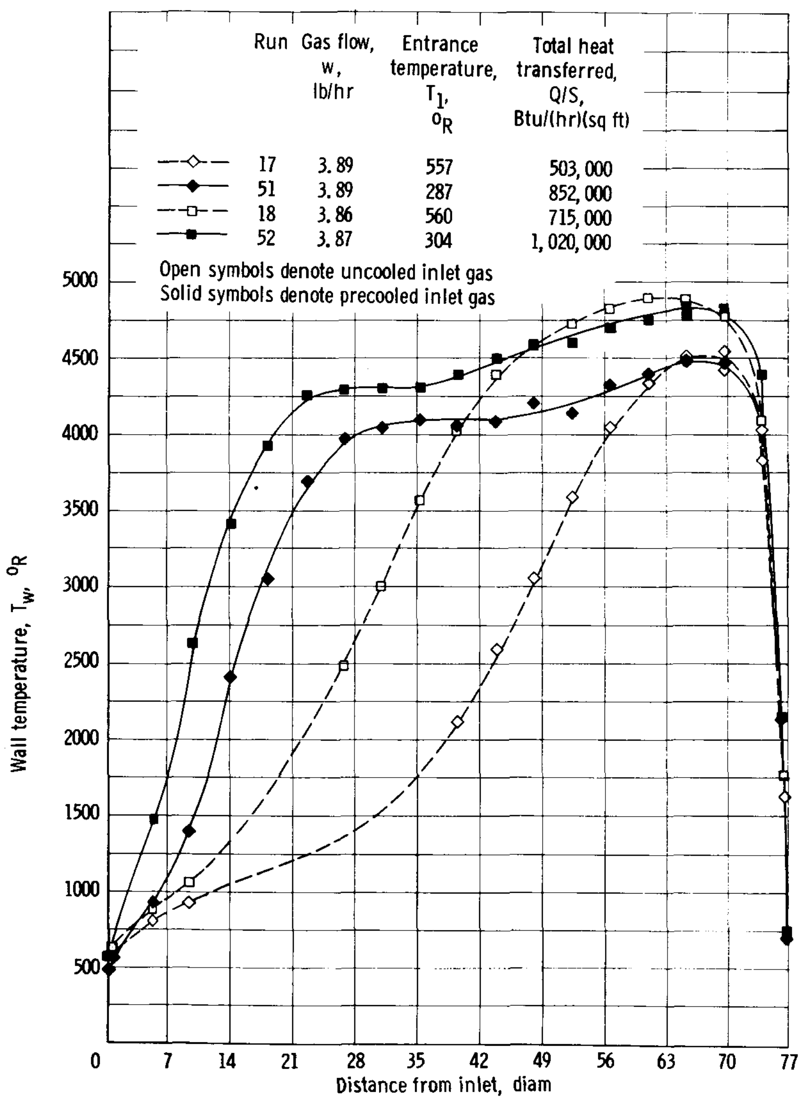

Figure 2. - Comparison of wall temperature distributions for cooled and uncooled inlet hydrogen based on flow rate and maximum wall temperature.

gradients at the entrance and the exit of the test section are the result of conduction losses to the connecting flanges, the mixing tanks, and the electrical connectors.

The heat-transfer parameters for the four hydrogen runs in figure 2 will be shown and discussed in the section Heat-Transfer Coefficients.

Friction Coefficients

As in reference 6, only average friction coefficients were measured. The friction coefficients for hydrogen and helium are shown in figure 3. The line representing the Kármán-Nikuradse relation between friction coefficient and Reynolds number for turbulent flow given by

$$\frac{1}{\sqrt{8\frac{f}{2}}} = 2 \log \mathrm{Re} \sqrt{8\frac{f}{2}} - 0.8 \tag{1}$$

and the laminar flow line given by

$$\frac{f}{2} = \frac{8}{\mathrm{Re}} \tag{2}$$

are included in figure 3 for comparison.

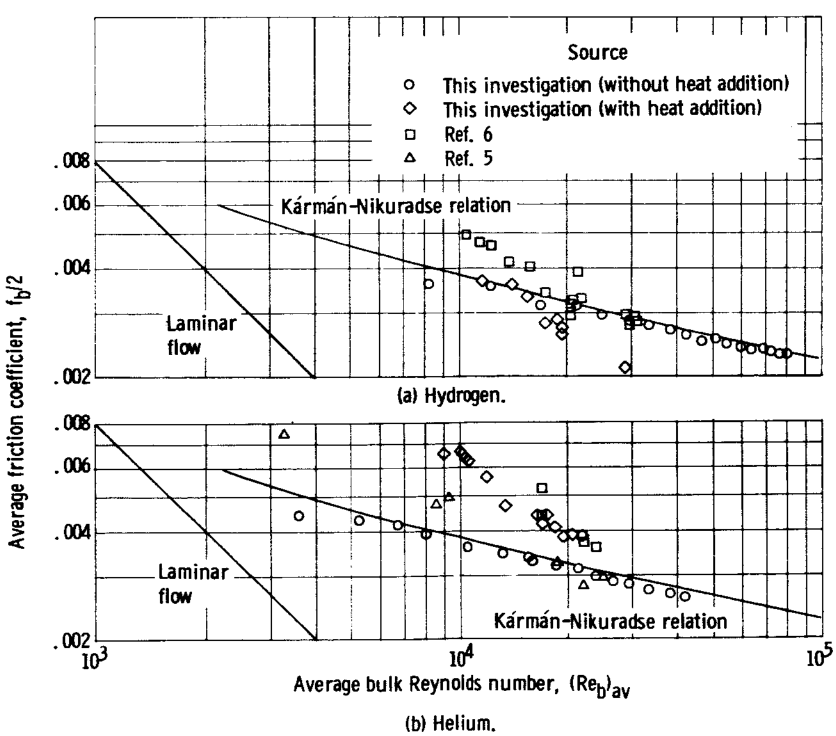

Figure 3. - Correlation of average friction coefficients. Viscosity and density evaluated at bulk temperature.

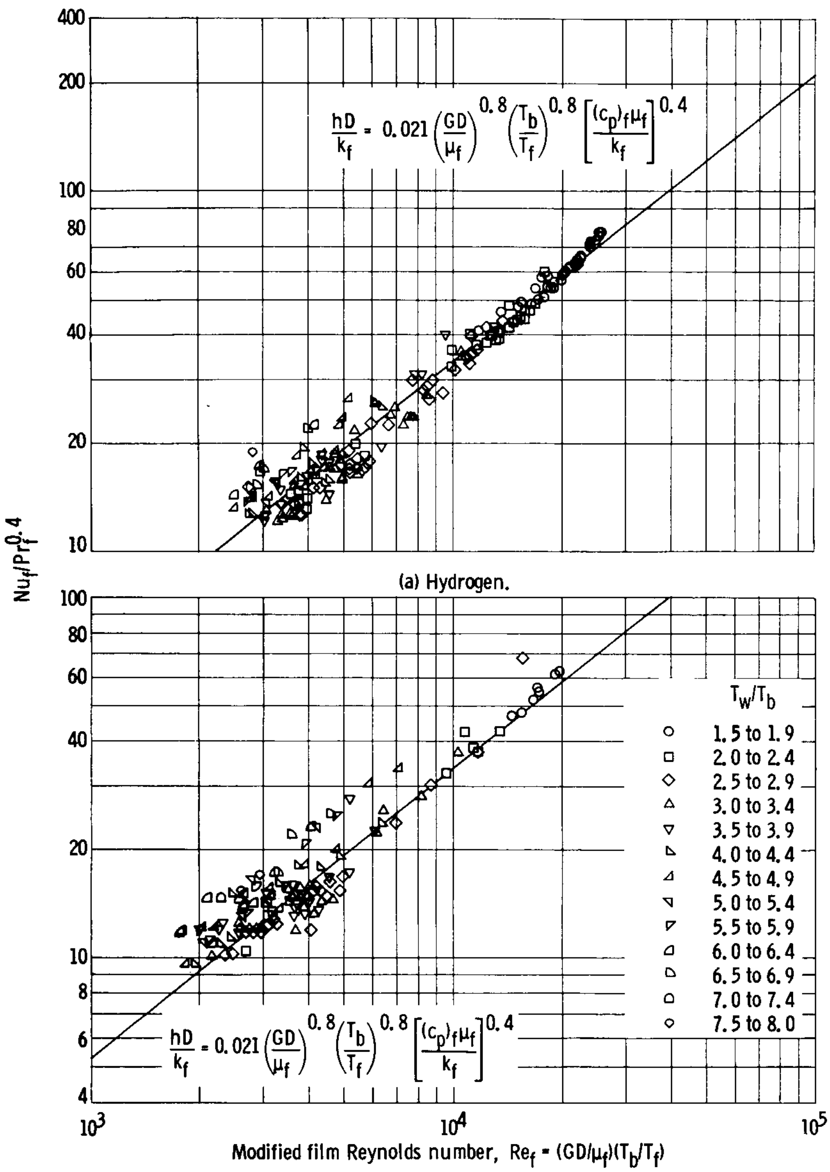

(a) Hydrogen.

(b) Helium.

Figure 4. - Film correlation of local heat-transfer coefficients using equation (3).

The hydrogen and helium runs without heat addition are in good agreement with the Kármán-Nikuradse relation. The friction coefficients for the helium runs with heat addition in this investigation agree with those of reference 6; neither agrees with the predicted line, however. The hydrogen friction data of this investigation fall below the hydrogen data of reference 6. The conclusion that must be drawn from figure 3 is that there is a need for further study of friction coefficients for conditions where the physical properties and density vary greatly in both the radial and axial directions.

Heat-Transfer Coefficients

In the present investigation as in reference 6, only local heat-transfer coefficients were calculated. The results of reference 6 indicate that, while some local heat-transfer data can be correlated to within ±10 percent by using the following equation

$$\frac{hD}{k_f} = 0.021 \left(\frac{GD}{\mu_f}\right)^{0.8} \left(\frac{T_b}{T_f}\right)^{0.8} \left[\frac{(c_p)_f \mu_f}{k_f}\right]^{0.4} \tag{3}$$

The data with large axial gradients in heat flux and surface temperature near the test-section entrance introduced deviations of as much as 30 percent from the correlation line. Data of the present investigation that have greater axial gradients in heat flux and surface temperature nearer the test-section entrance deviate as much as 60 percent from the correlation line (see fig. 4).

Reference 7 investigates the various methods of correlating hydrogen heat-transfer data proposed in references 2, 8, 9, and 10. The following correlating equations were proposed:

$$Nu_b = 0.025\, Re_b^{0.8} Pr_b^{0.4} \left(\frac{T_w}{T_b}\right)^{-0.55} \qquad \text{(ref. 2)} \tag{4}$$

$$h = C_2 G^{0.8} D^{-0.2} \left(\frac{T_w}{T_b}\right)^{-0.5} \qquad \text{(ref. 8)} \tag{5}$$

where C_2 is 0.048 for hydrogen and 0.020 for helium

$$Nu_b = 0.024\, Re_b^{0.8} Pr_b^{0.4} \left(\frac{T_w}{T_b}\right)^{-\left(0.29+0.0056 \frac{L}{D}\right)} \qquad \text{(ref. 9)} \tag{6}$$

along with a determination of reference temperature for evaluating the properties used in heat-transfer equations. The reference temperature T_x is defined by

$$T_x \equiv x\,(T_w - T_b) + T_b \qquad \text{(ref. 10)} \tag{7}$$

Both the hydrogen and helium heat-transfer data of this investigation and

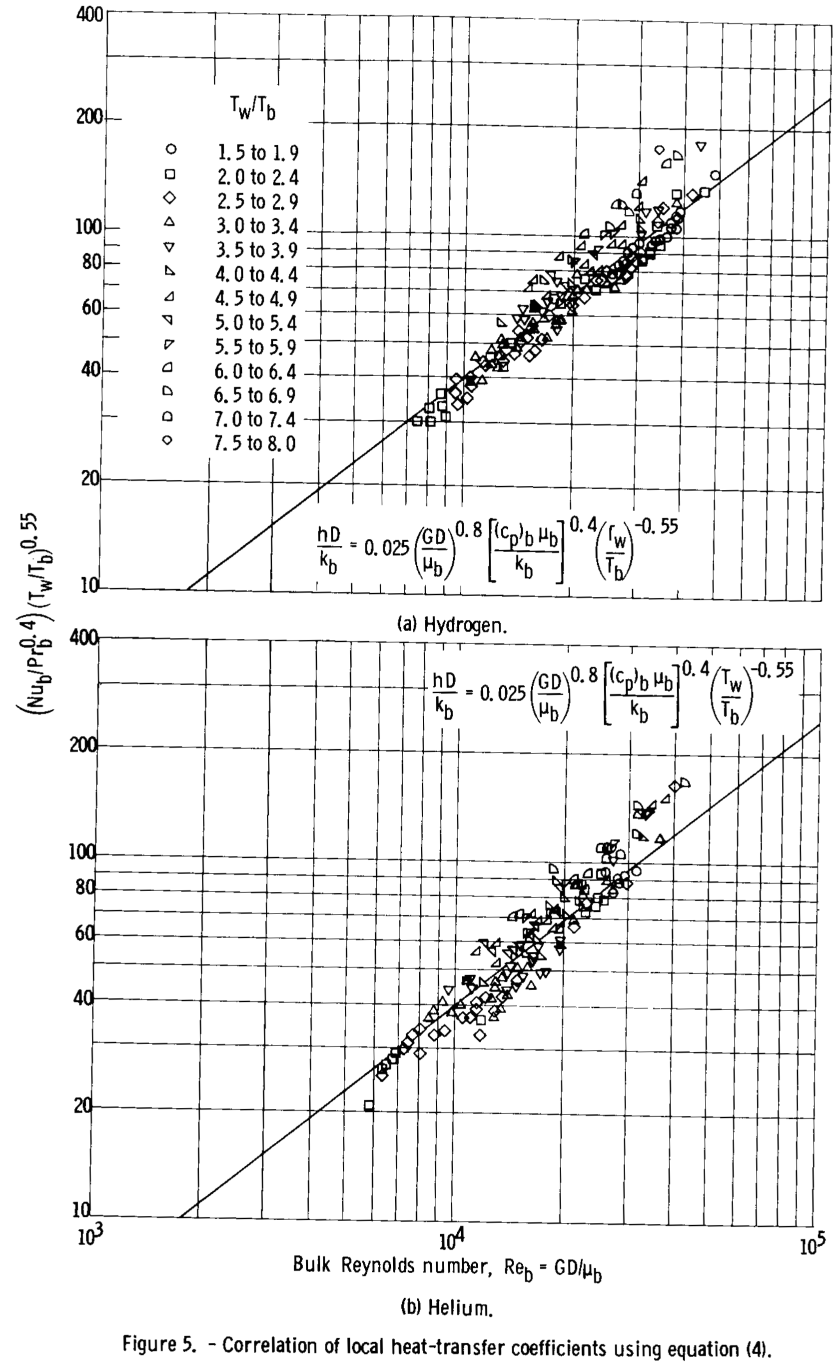

Figure 5. - Correlation of local heat-transfer coefficients using equation (4).

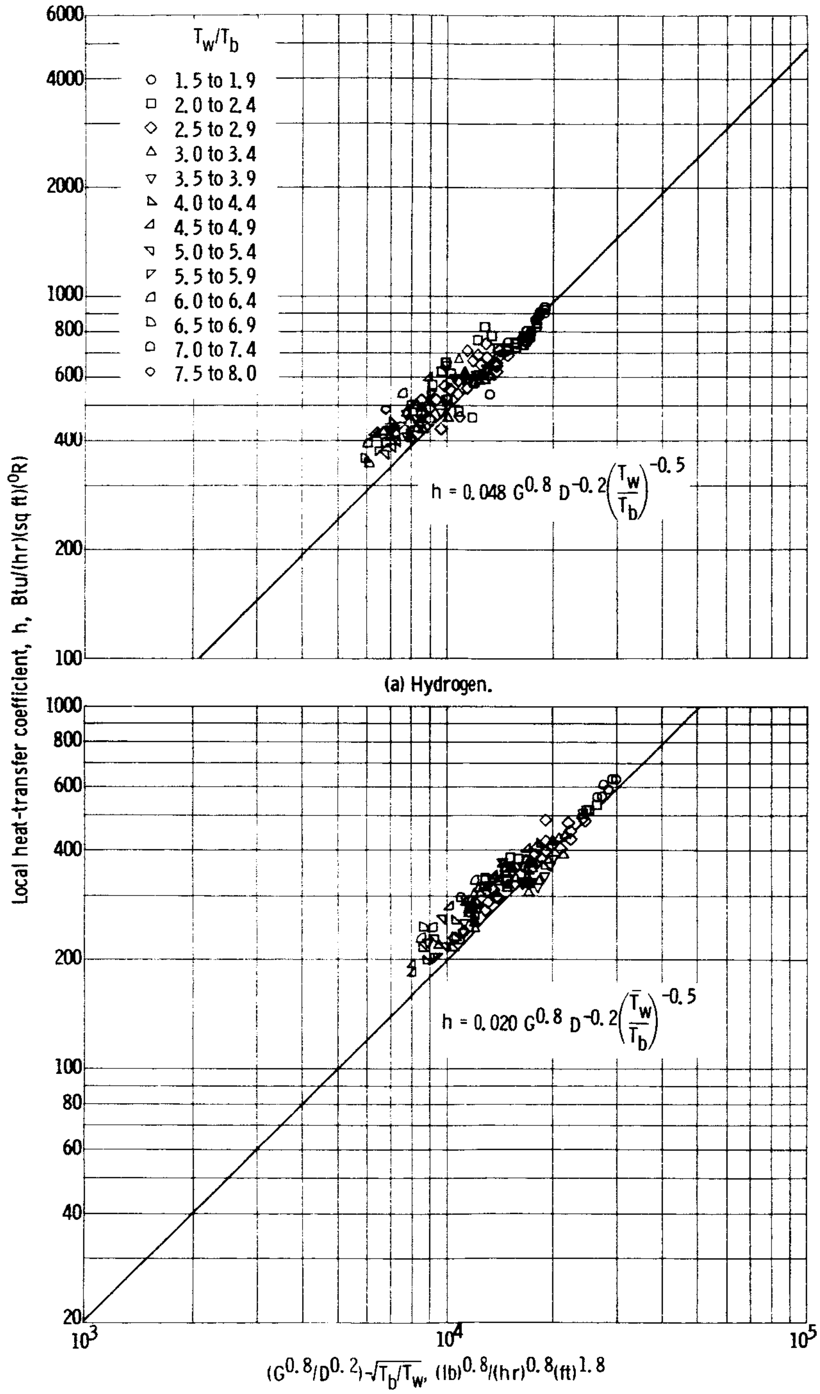

(b) Helium.

Figure 6. - Correlation of local heat-transfer coefficients using equation (5).

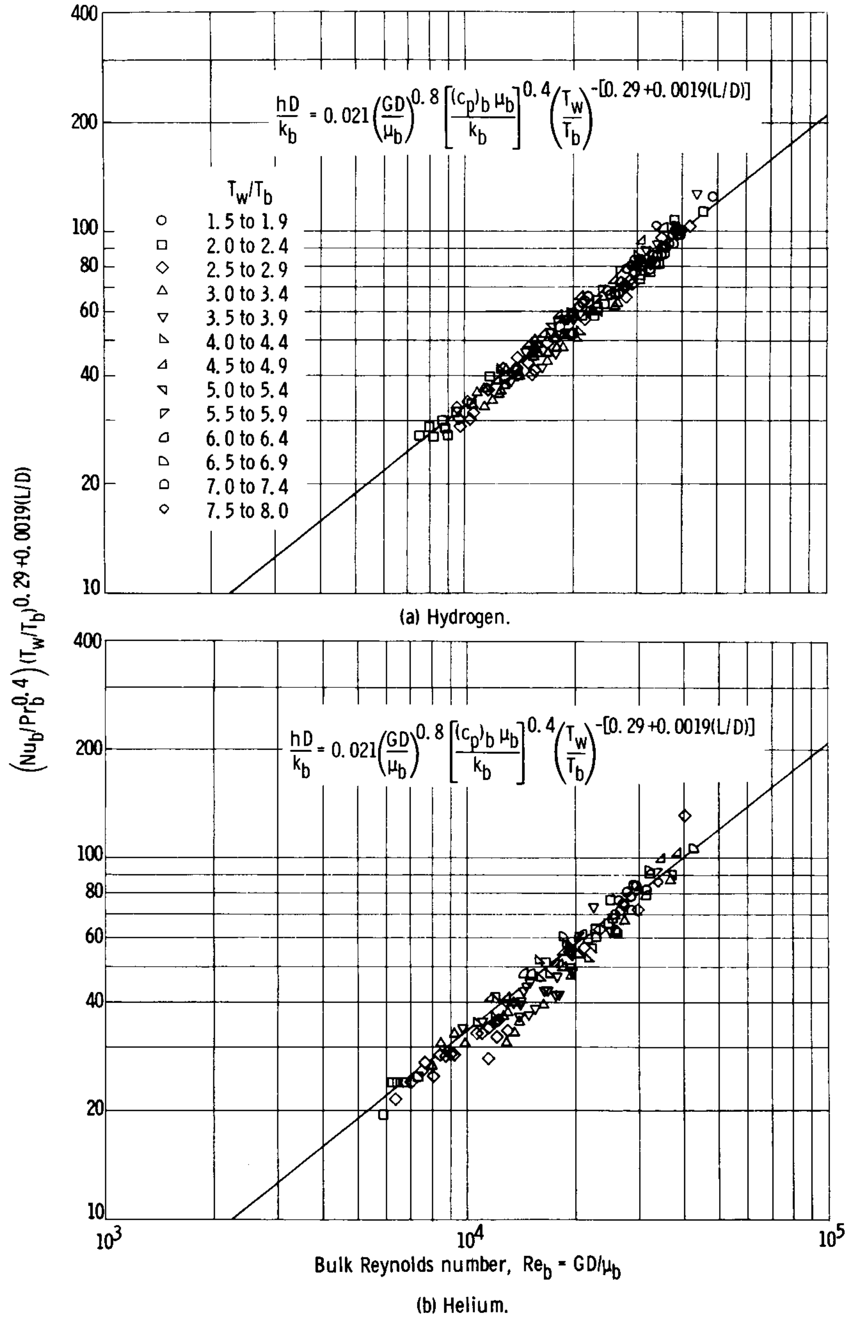

Figure 7. - Correlation of local heat-transfer coefficients using equation (8).

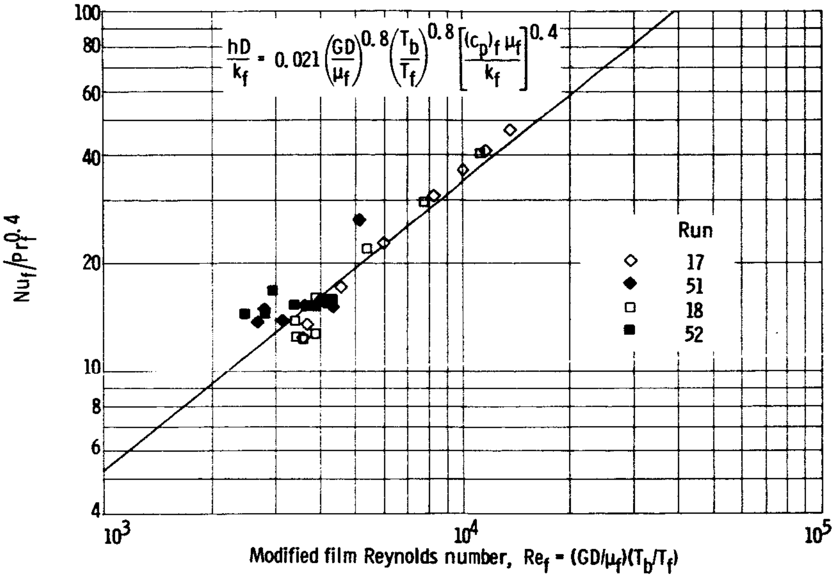

(a) Using equation (3).

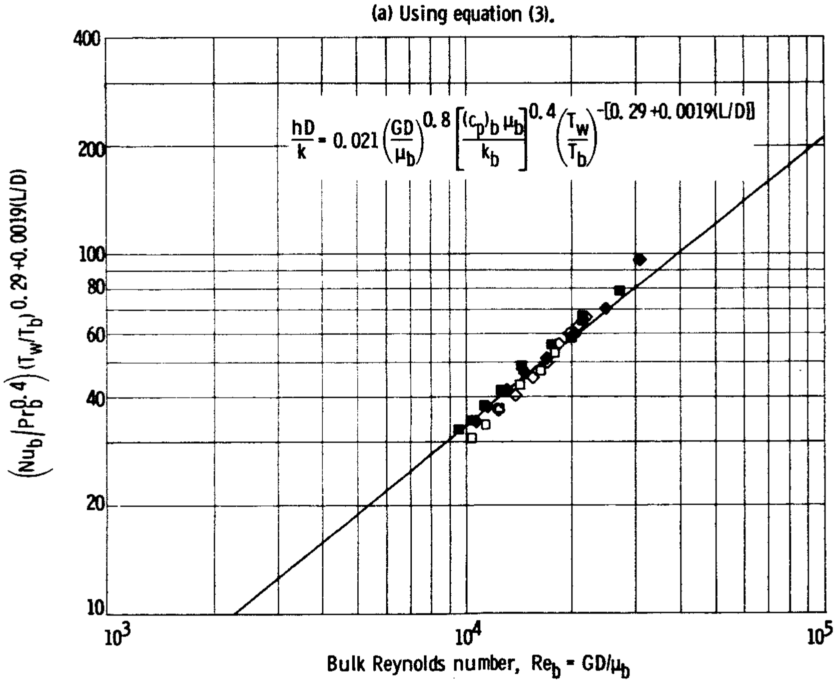

(b) Using equation (8).

Figure 8. - Correlation of hydrogen runs 17, 18, 51, and 52.

reference 6 correlated by equation (4) are shown in figure 5. There appears to be no improvement over the film correlation, merely a shift of the greatest amount of scatter from low to high Reynolds number.

Equation (7) could not be used because the range of Reynolds numbers presented in reference 10 was not low enough to include the uncorrelated data of either this investigation or reference 6. Reference 7 shows that this method does not correlate high Reynolds number data as well as equation (3) does.

Equation (5) attempts to correlate heat-transfer data by removing the properties from the conventional heat-transfer equation to simplify calculations. The heat-transfer data for hydrogen and helium are shown in figure 6. Both the hydrogen and helium data of reference 6 and this investigation fall as high as 40 percent above the correlation line. This cannot be corrected by increasing the constant C_2 in equation (5) because the data of reference 3 fall considerably below the correlation line.

A very good correlation can be obtained for the hydrogen and helium heat-transfer data of reference 6 and the present investigation with equation (6), as shown in figure 7. The exponent of the surface to fluid bulk temperature ratio was decreased from 0.29 + 0.0056 to 0.29 + 0.0019 L/D giving

$$Nu_b = 0.021\, Re_b^{0.8} Pr_b^{0.4} \left(\frac{T_w}{T_b}\right)^{-\left(0.29+0.0019\,\frac{L}{D}\right)} \tag{8}$$

which is useful for test sections where the length-diameter ratio is as high as 250, such as in reference 3. Both exponents worked equally well for data presented in this investigation and reference 6. The hydrogen data correlate better than the helium data with 90 percent of the hydrogen data falling within ±10 percent while 80 percent of the helium data correlate to within ±10 percent of the correlating line. The physical properties and density are evaluated at the bulk temperature. In this investigation and in reference 6, the maximum bulk temperature is about 2800° R, which is less than the temperature at which dissociation occurs at the pressures involved.

To show more clearly the trend of heat-transfer parameters when evaluated by means of equations (3) and (8), the parameters for the two noncooled and the two precooled wall temperature distributions of figure 2 are shown in figure 8. Figure 8(a) shows the parameter evaluated by using equation (3), and figure 8(b) shows the parameter evaluated by using equation (8). The improved correlation obtained by using equation (8) is quite striking.

SUMMARY OF RESULTS

The following results were obtained in an investigation of heat transfer to hydrogen and helium at pressures of 37 to 93 pounds per square inch flowing through a tungsten tube at surface temperatures up to 5300 and ratios of surface to bulk fluid temperature up to 8:

1. Some local heat-transfer data agree to within ±10 percent when cor-

related by using the Dittus-Boelter equation and chemically frozen (chemical reaction term not included) viscosity, thermal conductivity, and specific heat. These physical properties and density were evaluated at either the film or the surface temperature. Data obtained with large axial gradients in heat flux and surface temperature and large ratios of wall to fluid bulk temperature near the test-section entrance introduce deviations as great as 60 percent from the correlation equation.

2. A much improved correlation can be achieved for all the data by using $Nu_b = 0.021 \, Re_b^{0.8} Pr_b^{0.4} \, (T_w/T_b)^{-[0.29+0.0019\,(L/D)]}$ where Nu_b is the bulk Nusselt number, Re_b is the bulk Reynolds number, Pr_b is the bulk Prandtl number, T_w is the wall temperature, T_b is the bulk temperature, L is the distance from the test section inlet, and D is the inside diameter of the test section. The hydrogen data correlate better then the helium data do; 90 percent of the hydrogen data correlate to within ±10 percent, while 80 percent of the helium data correlate to within ±10 percent. The physical properties and the density were evaluated at the bulk temperature.

3. Friction coefficients without heat addition are in good agreement with the Kármán-Nikuradse relation. Friction coefficients with heat addition are in poor agreement with the Kármán-Nikuradse line.

Lewis Research Center
National Aeronautics and Space Administration
Cleveland, Ohio, October 26, 1964

APPENDIX - SYMBOLS

c_p specific heat at constant pressure, Btu/(lb)($^{\circ}$R)

D inside diameter of test section, ft

ΔE potential drop, v

f average friction coefficient

G mass flow per unit cross-sectional area, lb/(hr)(sq ft)

h local heat-transfer coefficient, Btu/(hr)(sq ft)($^{\circ}$R)

I current, amp

k thermal conductivity of gas, Btu/(hr)(ft)($^{\circ}$R)

L distance from test section inlet, ft

Nu Nusselt number based on local heat-transfer coefficient, hD/k

Pr Prandtl number, $c_p\mu/k$

p absolute static pressure, lb/sq ft

Q rate of heat transfer to gas, Btu/hr

Q_e rate of electrical heat input, Btu/hr

Re Reynolds number, GD/μ

S heat-transfer area of test section, sq ft

T_b bulk temperature of gas, $^{\circ}$R

T_f film temperature, $(T_w + T_b)/2$, $^{\circ}$R

T_w wall temperature, $^{\circ}$R

w gas flow, lb/hr

x parameter for specifying reference temperature; $T_x \equiv x\,(T_w - T_b) + T_b$

μ absolute viscosity of gas, lb/(hr)(ft)

Subscripts:

av average for complete test section

b bulk (when applied to properties, indicates evaluation at bulk temperature T_b)

f film (when applied to properties, indicates evaluation at film temperature T_f

w wall (when applied to properties, indicates evaluation at surface temperature T_w)

1 test-section entrance

2 test-section exit

REFERENCES

1. Humble, Leroy V., Lowdermilk, Warren H., and Desmon, Leland G.: Measurements of Average Heat-Transfer and Friction Coefficients for Subsonic Flow of Air in Smooth Tubes at High Surface and Fluid Temperatures. NACA Rep. 1020, 1951.

2. McCarthy, J. R., and Wolf, H.: The Heat Transfer Characteristics of Gaseous Hydrogen and Helium. Res. Rep. 60-12, North Am. Aviation, Inc., Dec. 1960.

3. Weiland, Walter F.: Measurement of Local Heat Transfer Coefficients for Flow of Hydrogen and Helium in a Smooth Tube at High Surface to Fluid Bulk Temperature Ratios. Preprint 126, A.I.Ch.E., 1962.

4. Durham, F. P., Neal, R. C., and Newman, H. J.: High Temperature Heat Transfer to a Gas Flowing in Heat Generating Tubes with High Heat Flux. TID-7529, pt. 1, book 2, Reactor Heat Transfer Conf., AEC, Nov. 1957, pp. 502-514.

5. Taylor, Maynard F., and Kirchgessner, Thomas A.: Measurements of Heat Transfer and Friction Coefficients for Helium Flowing in a Tube at Surface Temperatures up to 5900° R. NASA TN D-133, 1959. (See also ARS Jour., vol. 30, no. 9, Sept. 1960, pp. 830-832.)

6. Taylor, Maynard F.: Experimental Local Heat-Transfer and Average Friction Data for Hydrogen and Helium Flowing in a Tube at Surface Temperatures up to 5600° R. NASA TN D-2280, 1964. (See also Proc. of 1963 Heat Transfer and Fluid Mech. Institute, Stanford Univ. Press, 1964, pp. 251-271.)

7. Miller, John V., and Taylor, Maynard F.: Improved Method of Predicting Surface Temperatures in Hydrogen-Cooled Nuclear Rocket Reactor at High Surface- to Bulk-Temperature Ratios. NASA TN D-2594, 1964.

8. Simoneau, R. J., and Hendricks, R. C.: A Simple Equation for Correlating Turbulent Heat Transfer to a Gas. NASA TM X-52011, 1964.

9. Dalle Donne, M., and Bowditch, F. H.: High Temperature Heat Transfer. Nuclear Eng., vol. 8, no. 80, Jan. 1963, pp. 20-29.

10. Deissler, R. G., and Presler, A. F.: Computed Reference Temperatures for Turbulent Variable-Property Heat Transfer in a Tube for Several Common Gases. Int. Developments in Heat Transfer, Proc. Int. Heat Transfer Conf., 1961-1962, ASME, 1963, pp. 579-584.

TABLE II. - EXPERIMENTAL RESULTS

(a) Data for complete test section

Run	Total heat input, Q_e/S, $\frac{\text{Btu}}{(\text{hr})(\text{sq ft})}$	Total heat transferred, Q/S, $\frac{\text{Btu}}{(\text{hr})(\text{sq ft})}$	Gas flow, w, $\frac{\text{lb}}{\text{hr}}$	Entrance pressure, p_1, $\frac{\text{lb}}{\text{sq ft}}$ abs	Exit pressure, p_2, $\frac{\text{lb}}{\text{sq ft}}$ abs	Entrance temperature of gas, $T_{b,1}$, $^{\circ}$R	Exit temperature of gas, $T_{b,2}$, $^{\circ}$R	Average bulk temperature of gas, $(T_b)_{av}$, $^{\circ}$R	Average surface temperature of test section, $(T_W)_{av}$, $^{\circ}$R	Current, I, amp	Potential drop, ΔE, v
Helium											
32	540,000	325,000	4.72	5,888	2051	304	1555	930	2997	856	4.16
33	942,000	655,000	9.75	10,525	3217	252	1472	862	3376	1060	5.65
34	975,000	712,000	9.36	10,943	3195	269	1651	960	3784	1080	6.75
35	739,000	443,000	9.03	8,649	2842	254	1151	703	2793	1050	4.47
36	792,000	597,000	9.12	9,880	3004	260	1449	854	2947	1054	5.40
37	1,010,000	681,000	9.20	10,564	3133	266	1611	939	3511	1067	6.10
38	1,110,000	714,000	9.24	10,780	3162	272	1677	974	3731	1086	6.55
39	1,210,000	759,000	9.24	11,212	3270	280	1774	1028	3906	1108	7.15
40	1,330,000	886,000	11.73	13,350	4077	258	1635	947	3852	1168	7.70
41	442,000	295,000	6.06	6,065	2120	277	1160	719	2340	900	3.10
42	599,000	402,000	6.14	7,167	2127	256	1475	881	3036	904	4.39
43	750,000	462,000	5.91	7,621	2141	307	1729	1018	3502	932	5.35
44	863,000	504,000	5.94	7,973	2185	310	1654	1082	3744	960	5.95
45	1,030,000	562,000	6.11	8,535	2285	325	1998	1161	4105	994	6.70
Hydrogen											
46	642,000	437,000	4.91	5,371	2369	263	562	562	1603	1260	2.86
47	1,240,000	956,000	4.65	7,330	2539	272	1644	957	3264	1240	6.22
48	1,680,000	1,250,000	4.97	8,654	2887	277	1936	1107	3930	1306	8.40
49	2,230,000	1,180,000	5.14	9,850	3298	296	2350	1323	4483	1396	10.6
50	745,000	566,000	4.00	5,422	2110	277	1224	751	2343	1164	4.02
51	118,000	652,000	3.89	6,445	2153	287	1742	1015	3490	1172	6.50
52	1,460,000	1,020,000	3.87	7,135	2275	304	2028	1166	3958	1214	7.90

(b) Local outside surface temperatures of test section

	Distance from inlet, in.																				
Run	0	$\frac{1}{16}$	$\frac{5}{8}$	$1\frac{1}{8}$	$1\frac{5}{8}$	$2\frac{1}{8}$	$2\frac{5}{8}$	$3\frac{1}{8}$	$3\frac{5}{8}$	$4\frac{1}{8}$	$4\frac{5}{8}$	$5\frac{1}{8}$	$5\frac{5}{8}$	$6\frac{1}{8}$	$6\frac{5}{8}$	$7\frac{1}{8}$	$7\frac{5}{8}$	$8\frac{1}{8}$	$8\frac{5}{8}$	$8\frac{15}{16}$	9
	Wall temperature, T_w, $^{\circ}$R																				
32	499	580	940	1350	[a]1740	2441	2956	3396	3600	3676	3751	3794	3848	3897	3970	4032	3940	3794	3030	1695	601
33	[a]220	[a]320	755	1130	[a]1660	2647	3408	3903	4063	4063	4063	4087	4261	4411	4574	4637	4637	4562	3672	2020	640
34	520	620	1140	1840	3552	3588	3952	4186	4211	4280	4336	4461	4625	4790	4918	5006	4944	4714	3727	2100	650
35	[a]240	[a]260	[a]365	475	2103	2131	2227	2963	3648	3879	3903	3952	4091	4050	3965	3940	3842	3634	2905	1630	615
36	[a]260	[a]340	680	859	[a]1060	[a]1380	2171	2441	3242	3787	4050	4100	4186	4236	4311	4398	4411	4014	3396	1840	645
37	465	555	960	1520	2419	3135	3684	4112	4162	4162	4261	4323	4448	4587	4612	4676	4688	4562	3818	2015	675
38	515	600	1090	1759	2705	3468	3952	4186	4261	4261	4311	4448	4562	4663	4777	4828	4841	4663	3854	2090	690
39	495	585	1090	1822	3153	3842	4211	4311	4336	4323	4436	4612	4803	4905	4982	5040	5047	4905	4063	2215	719
40	495	585	1090	1822	2931	3630	4137	4273	4273	4286	4336	4511	4663	4816	4892	5008	5008	4944	4211	2222	715
41	[a]280	[a]320	490	575	[a]740	1981	2103	2182	2305	2774	3265	3552	3672	3708	3648	3612	3534	3313	2504	1320	575
42	[a]400	513	780	1098	2126	2362	2878	3432	3660	3794	3830	3830	3879	3940	4001	4050	4026	3860	2989	1640	600
43	555	675	1180	1779	2578	3194	3612	3915	4020	4069	4112	4174	4236	4361	4436	4417	4436	4298	3438	1879	635
44	600	738	1390	2118	2971	3576	3940	4137	4224	4236	4298	4411	4536	4612	4688	4726	4688	4587	3684	2035	640
45	700	890	1760	2620	3402	3989	4286	4436	4511	4574	4637	4803	4918	5034	5053	5034	5008	4869	4032	2250	675
46	[a]210	[a]240	[a]400	480	[a]570	[a]675	1958	1991	2025	2081	2086	2192	2266	2532	3194	3648	[a]3910	3927	3188	1528	655
47	[a]390	480	690	940	2215	2418	3147	3793	4062	4087	4075	4038	4124	4173	4248	4348	4435	4435	3988	2139	755
48	520	639	1310	2210	3289	3903	4235	4310	4260	4285	4335	4435	4586	4688	4739	4815	4841	4866	4586	2540	755
49	680	919	2230	3433	4335	4637	4675	4612	4624	4700	4841	4943	5072	5124	5176	5228	5280	5280	5034	3120	839
50	280	[a]330	520	1914	1969	2047	2086	2103	2204	2339	2878	3491	3878	4025	4025	3939	3854	3708	3064	1590	633
51	479	559	935	222	2407	3053	3684	3964	4062	4087	4062	4112	4211	4149	4323	4410	4498	4473	4038	2140	700
52	580	730	1470	2618	3396	3927	4248	4310	4310	4310	4385	4498	4586	4612	4688	4751	4841	4815	4410	2135	740

[a]Values from faired curves.

TABLE II. - Continued. EXPERIMENTAL RESULTS

(c) Data for increments

Increment	Local heat-transfer coefficient, h	Average outside surface temperature of increment, T_w, °R	Average bulk temperature of increment, T_b, °R	Increment	Local heat-transfer coefficient, h	Average outside surface temperature of increment, T_w, °R	Average bulk temperature of increment, T_b, °R
Run 32				Run 36			
1	135	815	317	1	100	596	263
2	217	1700	384	2	332	950	288
3	195	2550	515	3	335	1510	349
4	186	3340	686	4	323	2490	453
5	200	3650	887	5	282	3650	603
6	219	3770	1105	6	317	4070	791
7	233	3870	1330	7	360	4180	1008
8	242	3970	1555	8	369	4330	1235
9	248	3933	1769	9	377	4382	1457
10	-646	2996	1714	10	-333	3280	1508
Run 33				Run 37			
1	182	636	258	1	228	800	278
2	365	1378	301	2	323	1870	338
3	282	2770	400	3	285	3200	463
4	267	3836	543	4	292	4009	637
5	296	4070	717	5	342	4170	845
6	327	4080	906	6	357	4290	1070
7	332	4325	1101	7	362	4500	1297
8	324	4570	1299	8	379	4650	1528
9	335	4625	1495	9	402	4670	1759
10	-310	3613	1532	10	-708	3636	1743
Run 34				Run 38			
1	278	980	288	1	217	910	285
2	328	2150	363	2	321	2120	354
3	273	3556	500	3	293	3530	497
4	306	4138	683	4	324	4173	694
5	331	4250	892	5	353	4260	920
6	335	4410	1107	6	369	4390	1152
7	325	4680	1319	7	376	4610	1387
8	310	4940	1527	8	391	4770	1627
9	321	4942	1729	9	406	4831	1865
10	-450	3782	1740	10	-818	3738	1830
Run 35				Run 39			
1	-1102	350	242	1	152	960	290
2	492	630	249	2	330	2360	365
3	345	1500	309	3	295	3880	526
4	249	3013	415	4	340	4300	741
5	283	3780	570	5	370	4340	981
6	305	3950	759	6	383	4530	1227
7	325	3990	955	7	380	4830	1475
8	347	3970	1152	8	401	4990	1728
9	369	3830	1342	9	428	5031	1983
10	-898	2862	1292	10	-878	3902	1943

TABLE II. - Continued. EXPERIMENTAL RESULTS

(c) Continued. Data for increments

Increment	Local heat-transfer coefficient, h	Average outside surface temperature of increment, T_w, °R	Average bulk temperature of increment, T_b, °R	Increment	Local heat-transfer coefficient, h	Average outside surface temperature of increment, T_w, °R	Average bulk temperature of increment T_b, °R
Run 40				Run 44			
1	270	930	272	1	135	1130	327
2	361	2260	339	2	231	2440	414
3	336	3733	477	3	231	3620	592
4	374	4267	665	4	264	4110	830
5	408	4285	876	5	287	4240	1099
6	421	4440	1092	6	304	4370	1374
7	419	4720	1311	7	312	4560	1651
8	435	4910	1534	8	332	4680	1929
9	454	5027	1762	9	362	4702	2206
10	-692	4018	1756	10	-1050	3627	2099
Run 41				Run 45			
1	-307	440	269	1	102	1420	341
2	317	650	279	2	249	2910	448
3	249	1070	324	3	249	3996	662
4	237	1800	401	4	277	4420	927
5	219	2680	521	5	292	4560	1215
6	218	3400	680	6	311	4730	1508
7	234	3680	867	7	315	4970	1804
8	260	3650	1065	8	343	5050	2101
9	273	3560	1259	9	385	5004	2399
10	-524	2489	1257	10	-1145	3893	2273
Run 42				Run 46			
1	82	700	291	1	-428	356	260
2	294	1300	338	2	539	520	267
3	204	2450	440	3	467	710	292
4	211	3380	587	4	465	940	328
5	227	3760	774	5	461	1240	378
6	253	3830	980	6	475	1660	446
7	270	3900	1194	7	492	2290	544
8	286	4000	1410	8	456	3270	682
9	295	3996	1623	9	466	3893	854
10	-590	3044	1601	10	-288	3111	905
Run 43				Run 47			
1	143	980	321	1	-300	627	263
2	232	2130	397	2	474	1133	287
3	224	3230	551	3	421	2470	388
4	229	3898	753	4	395	3764	547
5	256	4060	984	5	440	4080	742
6	292	4140	1234	6	479	4070	951
7	303	4290	1494	7	535	4120	1169
8	317	4430	1753	8	557	4275	1394
9	340	4464	2011	9	577	4420	1618
10	-921	3387	1934	10	-305	3773	1686

TABLE II. - Concluded. EXPERIMENTAL RESULTS

(c) Concluded. Data for increments

Increment	Local heat-transfer coefficient, h	Average outside surface temperature of increment, T_w, °R	Average bulk temperature of increment, T_b, °R	Increment	Local heat-transfer coefficient, h	Average outside surface temperature of increment, T_w, °R	Average bulk temperature of increment, T_b, °R
Run 48				Run 51			
1	367	1090	299	1	238	830	299
2	433	2640	390	2	410	1782	365
3	447	3969	563	3	348	3253	502
4	498	4290	781	4	376	3951	690
5	546	4290	1015	5	408	4085	902
6	571	4410	1253	6	464	4110	1129
7	590	4620	1493	7	497	4170	1364
8	622	4780	1734	8	515	4330	1598
9	665	4850	1974	9	537	4470	1828
10	-586	4204	2015	10	-678	3711	1842
Run 49				Run 52			
1	366	1730	332	1	330	1227	332
2	487	3800	478	2	353	2884	437
3	538	4618	722	3	393	4000	629
4	594	4630	994	4	434	4311	868
5	634	4690	1272	5	477	4325	1124
6	668	4890	1552	6	505	4420	1384
7	708	5080	1833	7	530	4590	1643
8	759	5210	2115	8	563	4725	1900
9	824	5270	2394	9	604	4810	2155
10	-711	4662	2442	10	-878	4013	2155
Run 50							
1	-233	471	273				
2	479	596	282				
3	430	850	317				
4	418	1335	374				
5	395	2140	465				
6	373	3267	604				
7	385	3933	785				
8	420	4010	989				
9	453	3870	1193				
10	-248	2978	1259				

NASA-Langley, 1965 E-2664